Smart-surface: Large scale textile pressure sensors arrays for activity recognition

Jingyuan Cheng *, Mathias Sundholm, Bo Zhou, Marco Hirsch, Paul Lukowicz

German Research Center for Artificial Intelligence (DFKI), TU Kaiserslautern, Trippstadter Strae 122, D-67663 Kaiserslautern, Germany

ARTICLE INFO

ABSTRACT

In this paper we present textile-based surface pressure mapping as a novel, unobtrusive information source for activity recognition. The concept is motivated by the observation that the vast majority of human activities are associated with certain types of surface contact (walking, running, etc. on the floor; sitting on a chair/sofa; eating, writing, etc. at a table; exercising on a fitness mat, and many others). A key hypothesis which we validate in this paper is: by analysing subtle features of such interaction, various complex activities, often ones that are difficult to distinguish using other unobtrusive sensors, can be well recognised. A core contribution of our work is a sensing and recognition system based on cheap, easy-to-produce textile components. These components can be integrated into matrices with tens of thousands of elements, a spatial pitch as fine as 1 cm^2, temporal granularity of up to 40 Hz and pressure dynamic range from 0.25×10^5 to 5×10^5 Pa. We present the evaluation of the concept and the technology in five scenarios, through matrix monitoring driver motions at a car seat (32×32 sensors on 32×32 cm^2), a Smart-YogaMat (80×80 sensors on 80×80 cm^2) detecting and counting exercises, to a Smart-Tablecloth (30×42 sensors on 30×42 cm^2) recognising various types of food being eaten.

© 2016 Elsevier B.V. All rights reserved.

1. Introduction

Virtually all human activities involve interaction with surfaces. At the very least, due to gravity, some parts of the body need to be in contact with a supporting surface (ground, chair, bed, etc.). In addition, many actions involve hand interactions on surfaces such as tablets, tables or work benches. The work described in this paper is motivated by the hypothesis that most of such activities can be associated with characteristic spatio-temporal pressure patterns on the respective surface. A key insight is that such patterns are not limited to activities directly related to the respective surface (e.g. steps on the ground or hands operating something located on the table). Instead, vibrations, changes in centre of gravity and balance shifts propagate throughout the entire body, causing for example hand actions to influence the pressure distribution of the bottom of the feet on the ground. Thus, as will be shown later on, when a person is standing in front of a cupboard the pressure distribution on the bottom of the feet is different when reaching for the top shelves, for a middle or the bottom shelves (see Fig. 8). Similarly, when a person is lifting weights while standing, the rhythm and balance of the lifting motion is reflected in the pressure distribution on the ground. On a more direct level, cutting, poking on a plate or scooping food from it each produces a distinct pressure pattern on the table (Fig. 9).

---

* Corresponding author. Tel.: +49 631 20575 4181; fax: +49 631 20575 4020.
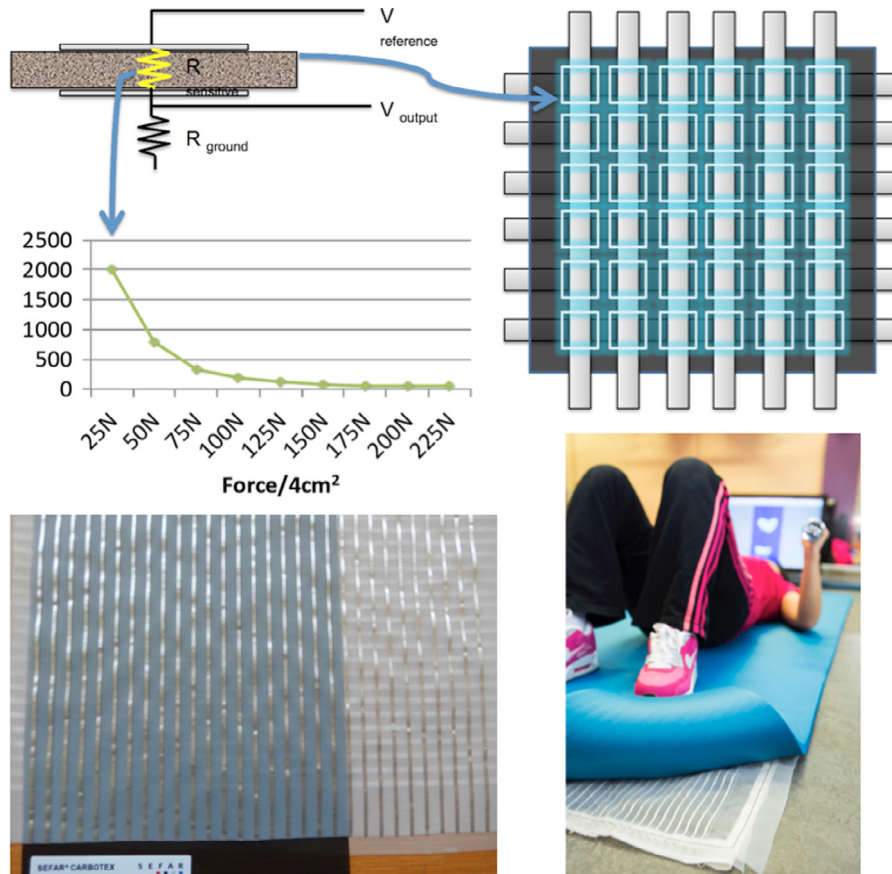*E-mail address:* jingyuan.cheng@dfki.de (J. Cheng).

Fig. 1. The pressure sensing matrix—physical model, implementation and usage in sport.

Table 1
Overview of applications with Smart-Surface for activity recognition. Results are given in person-dependent/person-independent recognition rate. Details of each application are given in Section 4. (p = participants).

Application	Sensor position	Sensor type	Collected data	Recognition rate
Pervasive control interface	on sofa	30 × 30 sensor matrix	6 p/60 × 15 gestures	96.0/90.0%
Posture recognition	on car seat	32 × 32 sensor matrix	8 p/180 × 9 postures	85.6/71.1%.
Tracking of sport exercises	in sport mat	80 × 80 sensor matrix	7 p/140 × 10 exercises	88.7/86.4%
Activity recognition	on floor	32 × 32 sensor matrix	11 p/220 × 7 actions	81.0/78.7%
Nutrition monitoring	on dining tablet	30 × 42 sensor matrix + 4 FSR	5 p/40 meals (15–40 min each)	87.1/71.4%

From the above considerations the contribution of this paper is threefold:

1. We present **Smart-Surface**, a cheap, unobtrusive textile pressure sensing matrix (see Fig. 1) that allows the acquisition of surface pressure distribution patterns with large temporal and spatial resolution and high dynamic range (1 cm^2 pitch, 40 Hz, from 0.25×10^5 to 5×10^5 Pa, details in Section 2).
2. We present a general processing chain (see Fig. 3) suitable for extracting activity related information from the signals of our sensing system.
3. We evaluate our system in 5 experiments (see Table 1): gesture recognition as a pervasive user interface on a sofa surface, posture/activity recognition on a pressure sensor matrix augmented car seat, sports exercise monitoring using a pressure sensitive yoga mat, upper body activity recognition using floor/carpet mounted pressure sensor matrix, and nutrition monitoring using a pressure sensitive table cloth.

The focus of our work is on demonstrating the diversity of activities that can be recognised with a relatively simple sensor. This includes activities that are (1) not obviously associated with surface pressure and/or (2) contain information that is difficult to recognise using other common unobtrusive sensing modalities such as inertial measurement units (e.g. balance of weight). Thus the detailed data mining techniques for each application are not the focus. Instead we present the general processing chain and the overall recognition accuracies. We have presented 4 out of the 5 applications as conference papers, in which the data mining details can be found [1–4].

Table 2
Comparison of existing digital pressure matrices.

Application	Modality	Node count	Analogue precision	Refresh rate
Commercial surface pressure mapping [24]	Resistive matrix	32×32	Discharging capacitor[a]	1 kHz
Shoes, gait analysis [25]	Opto-electronic	64 nodes	14-bit	1.8 kHz
Shoes, gait analysis [5]	Resistive	6 nodes	10-bis	100 Hz
Shoes, gait analysis [6]	Resistive matrix	48 nodes	12-bit	100 Hz
Seat, driver comfort [26]	Capacitive matrix	10×10	10-bit	100 Hz
Sitting posture [7]	Capacitive matrix	240 nodes	24-bit	90 Hz
Sitting posture [8]	Resistive matrix	16×16	Unspecified bit	10 Hz
Sitting posture [9]	Resistive matrix	42×84	8-bit	6 Hz
Bed, sleeper's vital signs and posture [27,28]	Resistive matrix	16×16	Unspecified	12 Hz
Bed, sleeper's posture and rehabiliation exercises [13,12]	Resistive matrix	64×128	Unspecified	Unspecified
Bed, sleep stage [14]	Resistive matrix	64×128	8-bit	1 Hz
Human computer interaction [21]	Resistive matrix[b]	42×48	8-bit	33 Hz
Humanoid robotics [29]	Resistive EIT[b]	16[c]	Unspecified	24 Hz
Smart-Surface	Resistive matrix	Up to 128×128	24 bit	40 Hz

[a] Discharging a capacitor is a low-end alternative to using an ADC [30].
[b] Electrical Impedance Tomography, a technique to reversely estimate the resistance distribution of a conductive material only from the rim [31].
[c] This is only the number of the physical electrodes; the calculated pressure mapping has higher resolution but is not specified by the authors.

1.1. Related work

When looking at related work we consider two aspects. First we look at research on pressure based sensing. Second we consider the broader area of activity recognition and discuss how the proposed large area pressure matrix is related to various common sensing modalities.

1.1.1. Pressure sensing

Resistive pressure sensors, sometimes also called resistive force sensors, recognise human activity through the force on an area. Wearable pressure sensors are used in shoes to analyse gait information [5,6]. Pressure sensor equipped chairs/seats can detect a user's posture [7,8] and be used in gaming [9], or recognise a driver's identity [10]. Furniture equipped with pressure sensors are used to recognise daily activities of the elderly [11]. Pressure sensor matrix equipped beds are used to recognise on-bed rehabilitation exercises or monitor sleep posture and stage [12–14]. Different kinds of pressure sensitive floors have been used for indoor positioning [15,16], gait/person identification [17–19,19], and human computer interaction [20,21]. Printed polymer-film pressure matrices are cheap in price and available on the market, but with very limited flexibility and no air permeability. In research and in products such as [22] or [23], optical interference is used to measure the surface pressure distribution of a piece of glass panel. The resolution and conversion bits are therefore solved by the widely well developed camera technology. However such technologies require a glass panel as the sensitive element, which greatly limits the application scenario possibilities.

Table 2 provides a brief overview over existing matrices regarding resolution, precision and refresh rate in comparison with our Smart-Surface. Overall our system stands out through the combination of high spatial resolution (up to 128×128 points with flexible, application specific pitch up to 1 cm), sampling rate (up to 40 Hz) and dynamic range (24-bits) which are achieved using a cheap unobtrusive textile setup.

1.1.2. Other sensing modalities

Overviews of activity recognition using various sensor types can be found in literature [32–35]. In general we distinguish between wearable and ambient sensors.

Wearable sensing systems can be with the users at all times no matter where they go. Inertial measurement units (IMU), which are small in size and have a direct link to activity, are extensively used at different body positions as wrist bands, bracelets, on torso or at pelvis, to recognise daily activities [36], gestures [37], for step and sleep monitoring [38], etc. However, IMUs pick up information only from the location where they are fixed to. To monitor complex activities where multiple parts of torso and limbs are involved, multiple IMUs on different body locations are needed, which is not very convenient for long term usage beyond lab environments. Also not all locations are well suited for attaching sensors regarding social acceptance (e.g. head and face) or for practical reasons (e.g. wet or sterilised hands). The most common wearable system with embedded IMUs, namely the smartphone, locates most of the time in the user's pocket or bag. Therefore it is not suitable for monitoring limb movements. Other IMU equipped wearable sensing platforms like smart watches [39], head mounted displays [40], or specific systems on rings, gloves or shoes [41,42], locate also only at a specific body location. Other wearable sensors include resistive [43] and capacitive smart textiles [44], microphones [45], magnetic sensors [46,47], RFID systems [48], biomedical sensors (electrocardiography, electromyography or electroencephalography) [49], etc., just to name a few.

Ambient sensing systems are hidden inside the environment. In general they are less obtrusive to the user but may require more installation and maintenance effort. The most successful category of ambient sensors are probably vision
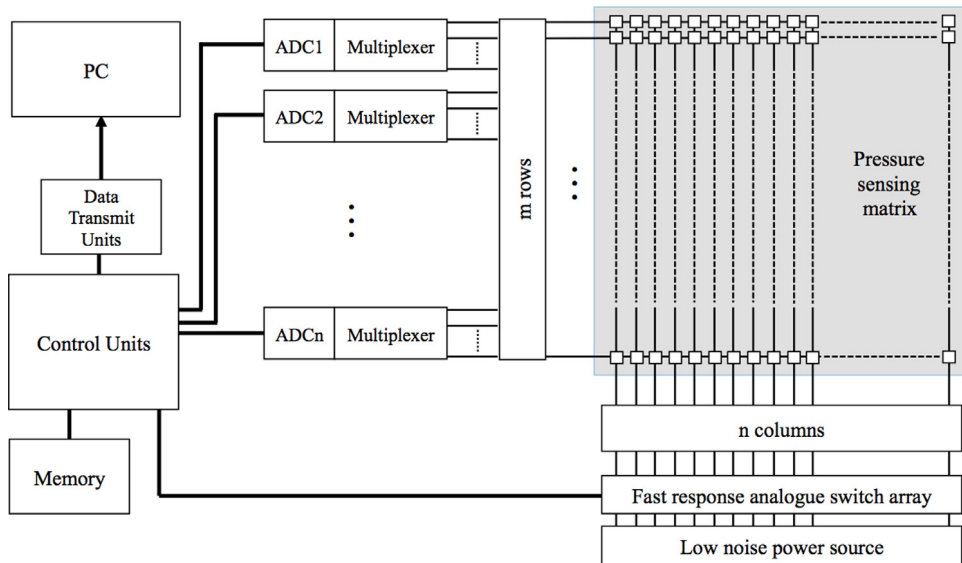
Fig. 2. System architecture.

based systems, including normal video cameras [50], thermal sensors [51], infrared cameras [52], and depth cameras such as the Kinect [53]. Cameras are also used in wearable systems (e.g. for automatic life-log [54]) and are included in most smartphones. While cameras can easily cover a large area like a room, there are challenges regarding occlusion, varying illuminations and privacy invasion. Besides cameras other ambient sensors have been proposed to monitor user activity. In [55] power consumption of kitchen appliances are used for monitoring the cooking habits. In [56] microphones are used to monitor bathroom activities. Signal strength [57] and proximity sensors [58] can be used to detect a user's indoor position and activity. They detect however human presence with higher confidence than the types of activities. Normally smart environments contain multiple sensing modalities (e.g. the Georgia Tech Aware Home [59]). Data from wearable and ambient systems can be fused to further enhance recognition performance [60].

Overall we see the core value of our Smart-Surface in being able to complement existing activity recognition systems with information that is difficult to obtain using other sensing modalities.

2. System architecture

A simple pressure sensitive element can be built by placing a pressure sensitive layer, e.g. carbon polymer foam between two electrodes. When force is applied to the sensor, the conductive layer gets compressed and the density of the conductive particles in the material increases, causing the resistance to drop. The resistive change is relative to the force applied to it and can be converted to voltage by a resistive voltage divider. The voltage signal can then be digitised by an analog-to-digital converter (ADC).

When multiple pressure sensors are arranged into a matrix, a grey scale image is created, representing the pressure distribution over the matrix. When touched by a person, the sensor matrix not only captures the overall force/weight, but also reveals detailed information like the shape and size of the contact area. With low-noise analogue design, high precision 24-bits ADCs and appropriate sampling rate, the matrix can produce a pressure image stream containing a lot of details about the person's activities.

We proposed a scalable and high precision architecture for the pressure matrix and corresponding control architecture [61], shown in Figs. 1 and 2.

The sensing matrix consists of three layers. The top and bottom layers are made of the same fabric, composed of evenly spaced parallel metallic stripes, separated by non-conductive polyethylene terephthalate. This fabric was designed by us in collaboration with SEFAR AG [62] and woven by SEFAR AG on normal textile machinery. The middle layer is a pressure sensitive semi-conductive fabric also produced by SEFAR AG (SEFAR CarbonTex [63]). The bottom layer is 90° rotated from the top layer, so that $n \times m$ cross-sections are created from n and m metallic stripes on the top and bottom layers respectively. Each cross-section acts as a pressure sensor and forms up one pixel in the pressure distribution image.

A field-programmable gate array (FPGA) controls the ultra-fast switch array and ADCs to drive the matrix and sample data from it. Each matrix column (ith from n) is switched on by enabling one switch and disabling the rest. The voltages on the m rows are then mainly related to pressure asserted to the m cross-sections on the ith column. These voltages are then passed to multiplexers and further fed into ADCs. At the next time step, the $(i + 1)$-th column is switched on and the readouts from ADCs now represent the pressure asserted to the $(i + 1)$-th column. By sweeping from the 1st to the nth column, an $n \times m$ pressure image is generated. When sweeping continuously, the images form up a data stream, representing the pressure

distribution and its change over time. This data stream is then sent to a computer via serial ports (UART-USB) with one physical USB cable. Our current implementation is capable of driving a maximum of 128×128 sensing points at 40 frames per second.

This architecture and implementation contribute to activity recognition with the following features:

High spacial resolution and proper sample rate: The majority of scenarios shown in this paper, feature a matrix with a spacial resolution of 1 cm^2, viz. 10^4 sensing points per m^2, providing extremely fine pressure distribution to reveal activity details. The 40 Hz sample rate is considered to be sufficient for typical human motions.

High sensitivity and wide dynamic range: We demonstrate by the various applications that the matrix is able to detect differences from very small (e.g. $\sim$100 g for an empty plate) to very high weights (e.g. $\sim$100 kg when a person stands on it). The concrete pressure at a single point depends on a lot of factors (not only the overall weight and the area of contact, but also the shape, softness and roughness of the contact surface). The mapping from pressure to voltage is both hysteric and non-linear. Thus it is hard to measure concrete sensitivity which will not be constant for all application scenarios. However, showing various application scenarios, we demonstrate that our matrix covers a large measuring range and meanwhile remains sensitive enough to detect both subtle and large human activities. A brief guess of dynamic range is achieved by putting different weights onto the sensing matrix. The result of one test is given in Fig. 1, where the measurement starts from 1 kg weight ($\sim$10 N) on a 4 cm^2 sensing area and reaches saturation at around 22 kg ($\sim$200 N), which corresponds to 0.25×10^5 to 5×10^5 Pa. This range mainly depends on the resistivity behaviour of the middle layer under pressure. In our case, the middle layer is made of woven semi-conductive polymer thread and the conductivity comes from the carbon-powder mixed into the polymer. We can thus expect that the measuring range changes with the percentage of carbon-powder mixed in, the thread's diameter, the weaving density, etc. To perform a quantitative study of their influence on the measuring range, different types of middle layer fabric must be manufactured, which is yet to be done because industry production need to be involved.

Scalability: The maximum number of the sensing points is limited by the FPGA pin numbers, ADC sample rate and data transmission techniques by design. Using state-of-art components, the upper limit of our architecture is $\sim 10^3 \times 10^3$. This means a coverage of 100 m^2 with a single system if the 1 cm^2 resolution is kept. This spacial resolution can also be scaled by changing the metallic stripes' separation, which can be between $\sim$0.5 cm and 0.5 m. To keep electrical performance, the resistance of the semi-conductive fabric needs to be raised when large pixel size, higher channel number or higher measuring range is desired. This can be adjusted by the percentage of carbon powder mixed into the threads and the percentage of semi-conductive threads woven in. The communication with a PC can be wireless through Bluetooth/WIFI with less pixel number for low-power consumption, or at a higher speed with Gigabit Ethernet or other high-speed bus like PCI Express for a higher pixel number. In a word, under our sensing architecture, the channel number, pixel size, coverage area, pressure measuring range, communication modality can all be scaled.

Comfort: Because all 3 layers are made of woven fabrics, the whole sensing matrix is soft, thin, flexible and air permeable, thus less obtrusion to the user. This ensures its long-time usage both in wearable and ambient applications.

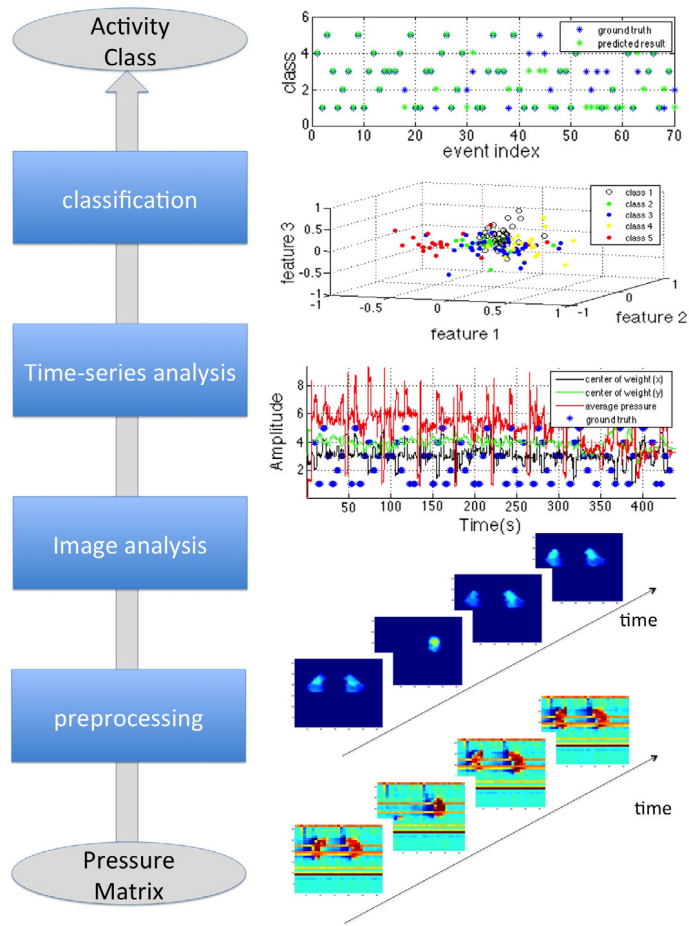## 3. Smart surface activity recognition workflow

From the sensor description above, it can be seen that the signal produced by the Smart-Surface is essentially an "image like" representation of the spatial pressure distribution at a given point in time. However, from the point of view of signal processing it differs from a "normal" image in several ways:

- Because the matrix can be considered as a resistor grid, where the resistors are not completely isolated from each other. A resistive change in one pixel also influences the nearby pixels, especially pixels in the same column since they are switched on at the same time.
- Every time the Smart-Surface is installed and used (e.g. put onto the ground), it is twisted slightly differently. Thus the default pressure distribution asserted by its own weight and folding changes.
- The sensor system is not an array of closely spaced pixels that produce a quasi continuous image but a grid where sensitive spots (junctions of the conductive lines) alternate with fairly large non sensitive spaces. This means that independently of the noise the image is not an accurate representation of the shape. Instead, depending on the alignment between the object exerting the pressure (e.g. the foot) and the grid, different shape and different overall absolute pressure value will be seen.
- Unlike in most computer vision applications, key information is often contained in relatively high speed (sub second) and subtle intensity (fully utilising the 24-bits dynamic range) changes.

On the positive side, unlike in classical image processing, there are no problems with background clutter and lighting conditions. There is also no scaling issue, although both shift and rotation invariance are important considerations.

For the recognition chain the above means that the following general steps are needed as a basis for application specific recognition method:

1. A pre-processing step that removes the Smart-Surface-specific noise described above.
2. A feature extraction step that emphasises abstract, shift and rotation invariant structural characteristics of the pressure distribution over the exact shape of individual objects visible in the image.

Fig. 3. General activity recognition workflow. Left: the steps in the processing workflow. Right: representing output after each processing step for application scenario Smart-Floor (Section 4.2.3), from bottom to top: 4 raw images from one event of the class *reach to the right side*, where some weight is moved from the left to the right feet (shown as two groups of heavily coloured pixels in each image) and then back; the 4 images after preprocessing; representing image parameters (centre of weight and the average pressure, scaled to be put into the same plot), accompanied by the ground truth; features from the time-series (Linear Discriminant Analysis[64] is used to reduce dimension and only the first 3 features after LDA are used in the plot); the predicted classes in contrast to the ground truth. (For interpretation of the references to colour in this figure legend, the reader is referred to the web version of this article.)

3. A temporal pattern extraction step based on the above features.

We have implemented a general recognition workflow for the Smart-Surface and used it in all our case studies. The workflow and typical output after each step is given in Fig. 3. The individual steps are described in more detail below.

3.1. Step 1: preprocessing

First, to compensate crosstalk within the resistor grid, a compensation term is calculated for every column of the frame as the minimum value of the column. Also in some experiments, an early hardware implementation was used and some columns or rows provided wrong values due to connection problems (as seen in bottom right subplots in Fig. 3). The values within these columns and rows are (1) much higher than it should be, (2) almost constant within the same column/row, (3) very different from the adjacent columns/rows. The sum of absolute difference of adjacent pixels within each column/row, divided by the sum of absolute difference of each pixel within that column/row to the next pixel within the adjacent column/row is then used as a measure to detect whether that column/row should be replaced by the adjacent columns and rows. For robustness the whole frame is filtered by a median filter.

Second, to account for difference caused by installing and usage, we calibrate the default distribution by removing the DC. The DC component for each pixel is calculated as the average value during the time when the matrix is not occupied.

Finally, to create a smoother spacial representation, each frame is up-sampled to twice the original size both on column and row. Up-sampling increases the pressure image resolution by interpolating intermediate pixels using bi-linear interpolation [65]. The higher resolution is not only visually smoother and more perceivable, but also contributes to more accurate calculation of image features (see next section), which leads to better classification results.

3.2. Step 2: feature extraction

For some applications, only a single major area is triggered on the pressure matrix, e.g. in Smart-Seat the main contact area is between the buttocks and the seat (Section 4.2.1). In other applications, there are multiple separated contact areas, e.g., in Smart-Floor (Section 4.2.3) two feet stand on the floor. As a consequence we characterise the spatial structure of the pressure pattern within a single frame on two levels. On one hand we consider the distribution over the entire sensor grid (single contact analysis). On the other hand we identify individual contact areas (e.g. caused by feet, hands) and characterise (1) the pressure within each area (using the same single contact analysis methods that we use for the sensor grid as a whole) and (2) the relationship between the different contact areas.

3.2.1. Single contact analysis

The analysis of a single contact area (or the entire sensor surface) is based on two types of features. First there are simple statistical parameters and second there are geometric image moments which provide a more sophisticated characterisation while being shift and rotation invariant.

Statistical parameters. Defining the pressure measured at the cross-section on the ith column and jth row in an $n \times m$ matrix at time t as $P(i, j, t)$ we consider the following parameters:

- Overall weight/force given by

$$W(t) = \sum_{i,j} P(i, j, t).$$ (1)

- Average pressure (mean or RMS) given by

$$\overline{P_{mean}(t)} = W(t)/A, \qquad \overline{P_{RMS}(t)} = \sqrt{\frac{\sum\limits_{i,j}(P(t, i, j) - \overline{P(t)})^2}{A}}$$ (2)

  where A is the contact area, for the whole image $A = n \times m$.

- Contact Area. By defining a threshold $P_{thres}(t)$, a pressure image can be divided into foreground (pressed, $P(i, j, t) \geq P_{thres}(t)$) and background (not pressed, $P(i, j, t) < P_{thres}(t)$). This threshold can be for example $\overline{P_{mean}(t)}$, $\overline{P_{RMS}(t)}$, or a value based on one of those (e.g. $\overline{P_{mean}(t)}/10$).

  Defining the set of pixels in a contact area as $[i, j] \in A_P$, where $P(i, j, t) \geq P_{thres}(t)$, the size of this area is then:

$$A = \sum_{[i,j] \in A_P} 1.$$ (3)

  Notice this A can also be used for the parameters above and below.

- Centre of Weight (the location of contact area) given by

$$\overline{x(t)} = \frac{\sum\limits_{i,j} P(i, j, t) \times i}{W(t)}, \qquad \overline{y(t)} = \frac{\sum\limits_{i,j} P(i, j, t) \times j}{W(t)}.$$ (4)

Geometric image moments. These moments describe the contact area's shape and distribution. Image moments are weighted averages of the intensity level of the pixels in the image, which effectively represent the global pressure distribution. Geometric image moments, however, are variant to translation, scale and rotation. Hu derived seven image moments that compactly describe the shape of the pressure distribution and are invariant to the above mentioned factors [66].

While Hu's moments are fast to compute, they are difficult to interpret. They are also not orthogonal and therefore contain redundant information. Teague introduced a new set of image descriptors by projecting the image into orthogonal radial Zernike polynomials [67], known as the Zernike moments. While more complex to compute, Zernike moments have been proven superior in image classification and more robust to noise [68]. They are invariant to rotation and the pressure distribution can be described accurately using a fairly low number of moments thanks to their orthogonal property. The lower order Zernike moments describe the general shape and the higher order moments can be used to distinguish smaller details. Due to the orthogonality of Zernike moments, the classification accuracy normally grows with the training dataset's size. Because current work focuses on scenario exploration, the dataset in most of the experiments is rather small (10–20 repeats from 5–10 test subjects). Even though Zernike moments can be of a higher number than the Hu's moments (as many as wanted against maximum 7), they might lead to overfitting.

3.2.2. Multiple contacts analysis

Image segmentation is used to split the image into the relevant portions. The image parameters described above are then calculated for each individual contact area. Also the number of contact areas and the combination information from

multiple areas are included, e.g. the distance between weight centres of the different areas, the ratio of weights, etc. To split the contact areas, the image can be pre-defined into several regions and contact areas are then extracted from each region. For example, the centre of weight can be used to split an image into the right and the left regions. If the shape of contact area is well known, template matching can be used. For example, regarding the round footprints left by dishes and glasses on the Smart-TableCloth (Section 4.2.4), Atherton and Kerbysons's circle detection algorithm [69] is applied. For more complex and dynamically changing areas, unsupervised image clustering based on K-means [70] or information bottleneck [71] can be used.

3.3. Step 3: time-series analysis

For many activities key discriminative information is often contained in subtle temporal characteristics of the pressure distribution. We have found that detecting such temporal characteristics by direct analysis of pressure image sequences is difficult due to various noise sources described above (such as shifts of the contact surface with respect to the grid structure). Instead, temporal analysis is best performed on the features described in the previous sections, which are specifically designed to separate noise artefacts from information related to human activities.

Thus, temporal analysis is applied to multivariate time series, in a way similar to what is usually done with IMU signals. Both time domain features (e.g. signal mean, standard deviation and, zero cross rate) and frequency domain features (e.g. main frequency, frequency centroid, and energy) can be used.

When a specific action generates a distinguishable and repeatable pattern, template matching becomes feasible. To handle actions at different speeds, dynamic time warping (DTW) is used, which finds the optimal distance between two time-series [72]. The DTW distance to a template can be used both as a feature in classification and/or as a measure to spot activities from data stream. Overall, the specific type of analysis is application dependent.

3.4. Step 4: classification

The final classification is performed on a combination of spatial and temporal features. Both, the selection of the features and the specific classification algorithm are application dependent. In most cases we have found that normalisation of the features using mean and standard deviation from the training dataset can significantly improve the results.

4. Scenario exploration and evaluation

We have conducted a series of studies to evaluate the Smart-Surface, exploring various activity recognition scenarios in people's daily lives, both as furniture cover and on the floor. The evaluation proceeds from explicit interaction with a textile surface when it is used as an "on furniture" user interface, through actions of body parts directly in contact with the Smart-Surface (e.g. different postures being sensed on a chair), to scenarios that demonstrate the ability of the system to detect activities through motion propagated to different body parts and balance changes.

4.1. General experiment workflow

For each application scenario, we designed experiments and recorded data from the Smart-Surface. All these experiments share the same workflow.

For each experiment 4–10 persons have been invited, mainly healthy master and Ph.D. students in computer science. Before each experiment, an experienced person (supervisor) explained purpose/content of the experiment and how the system works to each participant (subject).

The experiments contained a set of predefined activities, each repeated by the subject for at least 10–20 times. In some experiments, the activities were simple and could be performed within a certain time (e.g. to open the left/right cabinet), the instructions on when and what activity to perform were then given by a computer in front of the subject. The program ensured that these activities are performed in a random order and also kept a log on what activities have been performed when (automatic labelling). In other experiments, the activities have been more complex and were embedded at random times with random duration in a long data stream (e.g. stirring the noodle while eating). These experiments have been video recorded and the labels were generated later manually based on the video. The subjects have been given as much freedom as possible to ensure a high data variety. They have been provided with high-level activity instructions rather than a detailed description on how to perform them. During the complex experiments, they were also allowed to do other things, irrelevant to the predefined activities.

The data and the labels from multiple subjects were then put into the activity recognition workflow to evaluate the Smart-Surface's performance.

4.2. Smart-SofaCloth as pervasive control interface

As a first evaluation we considered a situation where the user explicitly interacts with the Smart-Surface. The idea is to transform the surface of furniture (e.g. sofa) into a user interface that would allow people to control for example a TV or
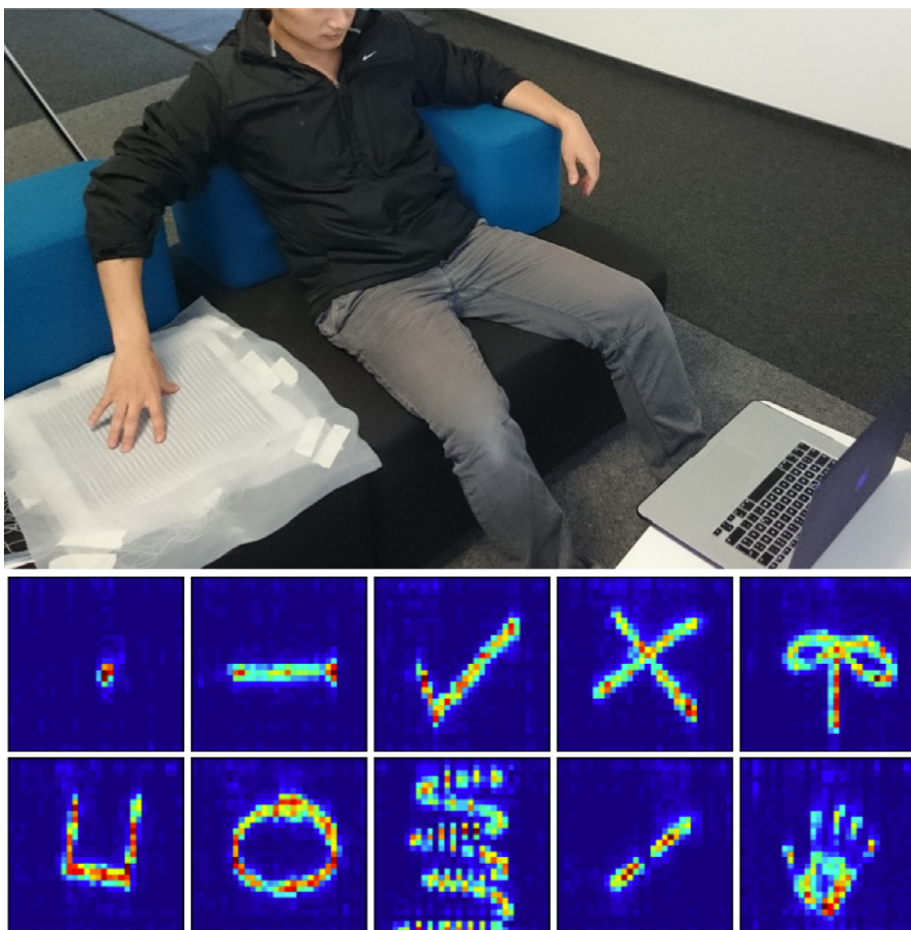
Fig. 4. A user draws gestures on the sofa. Images below show aggregated frames of the typical gestures studied: *tap*, *swipe*, *tick*, *cross*, *plant*, *glass*, *plate*, *water*, *pinch*, and *palm*.

the whole smart home. Note that the aim of this study is not to demonstrate the quality of the user interface (which would require a full appropriate user interface) but to test the ability of the system to recognise different pressure patterns in the "simple" case where these are explicitly and consciously generated by the user. Equipping furniture surface with pressure matrix not only enables a computer to passively detect human activities, but also the human to actively input information into the computer.

We performed a feasibility study by placing a 30 × 30, 1 cm^2 spatial resolution textile matrix on the seat of a two-seated sofa (see Fig. 4) [4]. Six participants were asked to sit next to the matrix and perform touch gestures on it, including 9 typical gestures for touch interfaces (*tap*, *double tap*, *swipe left/right/up/down*, *two finger pinch in/out* and *palm*) and 6 easy-to-draw symbols that reflect different commands in a home automation scenario (*tick* and *cross*, *glass*, *plate*, *plant*, and *water*). All gestures were repeated during 10 rounds in random order, instructed by text, illustration and voice command from a notebook.

In total 17 features are calculated for each gesture, including Hu's moments on the aggregated image frames, average blob count, number of threshold crossings, and difference between the centre of weight at starting and ending positions. Those features are used to train a bagging ensemble of 100 classification and regression trees (CARTs). Based on 5-fold cross-validation, a 96% person dependent and a 90% person independent accuracy are achieved.

4.2.1. Smart-CarSeat for monitoring the driver's activity

When cars get smarter, it is important for them to be aware of the driver's mental as well as physical status. A pressure matrix built into seat can measure how the driver sits and moves, which might be linked to uneasiness, discomfort or stress [73,74]. Such postures and actions could even be used to predict traffic context and the driver's intentions. Dangerous manoeuvres such as reaching to the back seat or to the car floor (e.g. to take care of a child or to pick up a dropped mobile phone) could also be detected. We use such scenarios to show the next step of conscious monitoring from pressure patterns described in the previous section. Thus we analyse pressure patterns that result from direct contact with the relevant body part, but are not generated by the user specifically for the purpose of interaction with the system.

Fig. 5. The textile pressure matrix as a seat cover. Postures from top left to bottom right: *sit normal*, *lean front*, *lean right*, *lean left*, *look back right*, *look back left*, *reach back right* and *touch floor*.

We integrated a 32×32, $1\,cm^2$ spatial resolution pressure matrix into a car seat cover and invited 8 subjects to perform 8 different postures/actions in our lab environment (see Fig. 5): *sit normal*, *lean left*, *lean right*, *lean front*, *look behind left*, *look behind right*, *reach back right* and *touch floor*. As a 9th class we included *vacant seat*. The activities are repeated in 20 rounds and guided by a computer program.

Every recorded frame is smoothed with an 8×8 spatial Gaussian filter to suppress noise and up-sampled from 32×32 to 64×64. Each frame is then normalised using the overall weight and the first 16 Zernike moments were calculated. Only Zernike moments with positive repetitions are used because of symmetry. We also calculate the first 16 Zernike moments from the difference frame, which is the current frame minus the frame while sitting normally. This emphasises the change in posture. Because rotation also contains important information on leaning to the left or right side, both the real and the imaginary components of the Zernike moments are used.

With a 50 tree Random Forest Classifier, the person dependent accuracy is 85.8% based on 10-fold cross-validation and person independent accuracy is 71.6% based on leave-one-out validation.

4.2.2. Smart-Mat for gym exercises evaluation

Sport is an important part in modern life. We implemented an 80×80, $1\,cm^2$ spatial resolution textile matrix as a smart gym mat and demonstrate that it can recognise 10 different exercises and count repetitions (see Fig. 6) [1]. These exercises consist of coordinated movement of different body limbs that are difficult to capture with a single body worn sensor. Compared with the car seat experiment we are now looking at more complex pressure distributions. In addition the pressure changes are not always caused by the body parts directly in contact with the Smart-Surface.
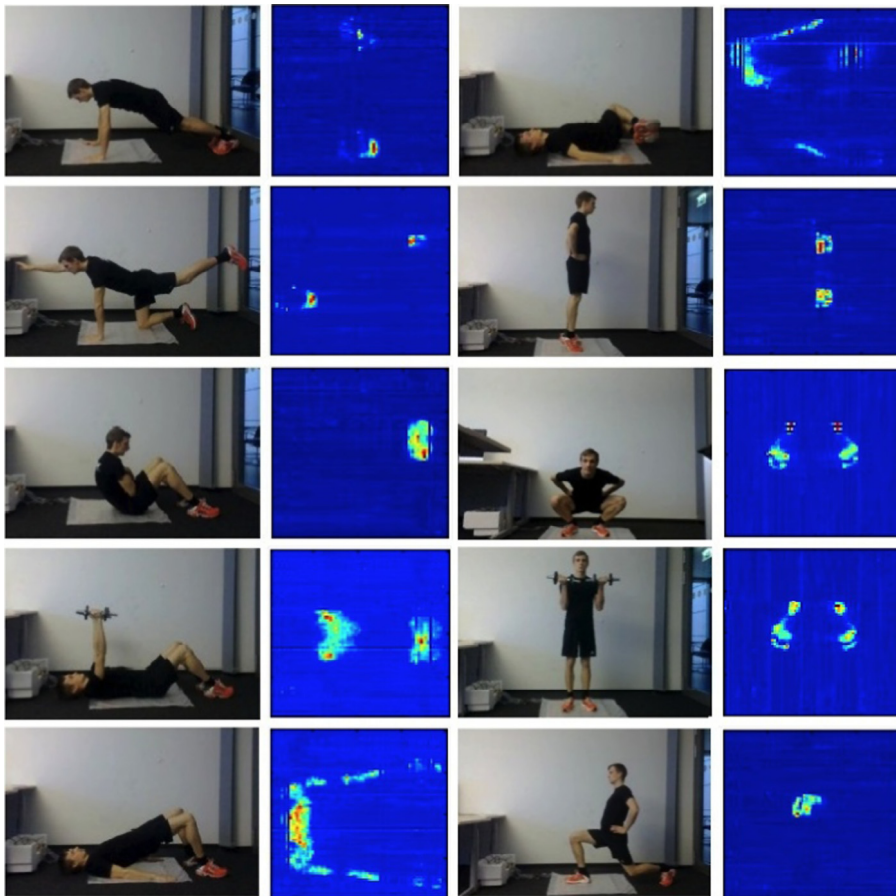
Fig. 6. Exercises performed in the experiment: *push-up*, *quadruped*, *abdominal crunch*, *chest press with dumbbell*, *bridge*, *segmental rotation*, *calf raise*, *squat*, *biceps curl with dumbbell*, and *lunge*. The pictures on the right are typical frames corresponding to the exercise.

Seven healthy participants were invited to perform 10 predefined sport exercises on the sensor mat. The exercises were selected from a pool that is recommended by experts at Mayo Clinic [75]. Each exercise was repeated 10 times per set and each set was performed 2 times per subject. To create a larger variance, the participants were asked to perform the first set at a fast tempo and the second set at slower tempo. The experiment has been video recorded and the starting and ending points of each exercise were manually labelled.

The pressure images are up-sampled from 80×80 to 160×160 and 10 image parameters are calculated for each frame: total weight, contact area, average pressure, and Hu's 7 Moments. These parameters are all invariant to translation and rotation, so that the user's position on the mat will not influence the recognition result. From the 10 image parameters 70 temporal features are calculated. Using a k-NN classifier we achieve 88.7% and 82.5% for person independent and dependent accuracy, respectively. Because in each set only one exercise is repeated continuously, the accuracy can be further pushed to 86.5% (person independent) with majority voting over the complete set.

In order to count the repetitions, templates for each exercise are created. The parameters in time-series of multiple repeats of the same exercise are aligned and scaled to their median length. Those were then averaged and used as the exercise template. To each exercise template, 10 weights are assigned to the 10 parameters. Data lying in a sliding window is compared with the exercise templates at every step using dynamic time warping in 10 dimensions. The template weights are used to emphasise the dimensions containing more relevant information. The inverse of the weighted DTW distance is considered as "match". A high match indicates the time when the data stream has a high similarity to the exercise template, thus considered as one repetition of the exercise (detected event). The peaks are detected robustly using hysteresis thresholds. If the detected event lies within the starting and ending points of the label, it is considered as a true positive.

User independent leave-one-out cross-validation is performed where the exercises for each subject are counted using templates from the other subjects. Since people have different body sizes and styles of performing exercises, for each subject, the template with the best DTW match from other subjects is automatically chosen. The achieved detection rate is presented in Fig. 7 as F_1-score [76], which can be interpreted as a weighted average of the precision and recall. The counting performance is 80%–100% for most subjects and most exercises, with the average counting accuracy of 89.9%.
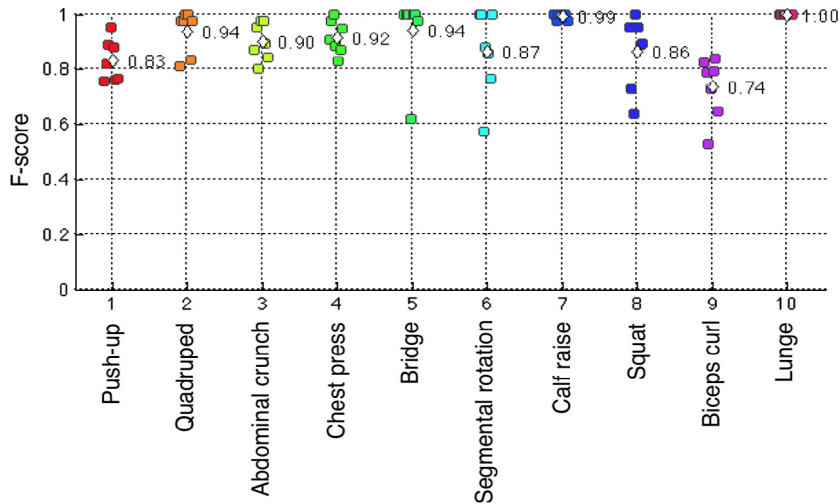
Fig. 7. Exercises' F_1-scores. Each dot represents the counting performance of one exercise type of one subject. The numbers show the average performance of each exercise type.

Fig. 8. Experiment setup and 7 activities, open/look-into/close drawers and doors of *upper left*, *upper right*, *middle*, *low*, *bottom*, *left* and *right*.

4.2.3. Smart-floor for upper body activity recognition

With a spatial resolution of a few centimetres, human feet can be detected and therefore a person's position and facing direction. Also subtle arm and torso movements propagate through the feet onto the ground. As an example, we demonstrate that by using a pressure matrix on the floor, we can recognise with which drawer a user interacts within the 3D space and that the interaction itself carries sufficient information to identify the person [2].

We put a 32×32, $2\ \text{cm}^2$ spatial resolution pressure matrix on the floor in an office kitchen and asked 11 participants to stand on the matrix and open 7 different drawers and cabinets (see Fig. 8). These actions were chosen because these positions are related to objects often used in our daily life. For example in a western kitchen, the cabinets on the top are often used for dishes, the drawers in the middle for cutlery and the cabinet on the bottom for kitchen waste. The activities were repeated in 20 rounds, instructed by a computer in random order. The subject was asked to step away from the matrix after each round to avoid a fixed standing position.

Each recorded frame is smoothed with a 4×4 spatial low-pass filter and up-sampled to 64×64. The two feet are segmented from the pressure image using thresholding. Binary masks are created for the left and right foot. Parameters such as area and centre of weight are then calculated for each frame and also separately for the masked segments. Based
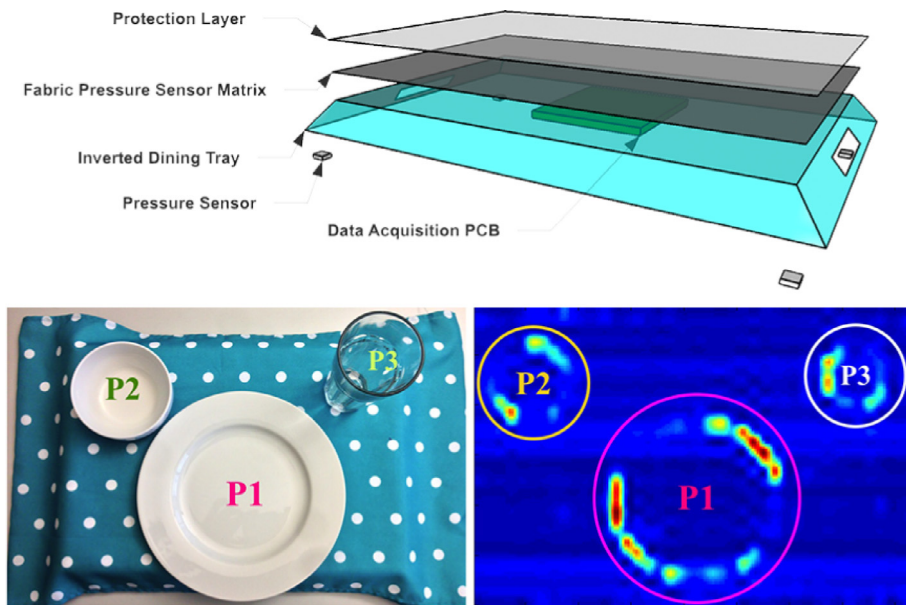
Fig. 9. The pressure sensor matrix detects the position of the plate, bowl and glass on the dining tablet.

on the absolute difference between consecutive frames, every action is divided into 3 phases: *opening the drawer/cabinet*, *looking inside* and *closing*. Temporal features such as mean, minimum, maximum are calculated from the image parameters within the 3 phases. Using a Random Forest classifier, we achieve a person dependent accuracy of 81.0% using 10-fold cross-validation and a person independent accuracy of 78.7%. When the 7 actions are further mapped into 5, emphasising the main directions, viz. *up*, *down*, *left*, *right* and *middle*, the person dependent and independent accuracy grows to 86.3% and 83.6%, respectively. To recognise people's identities, another Random Forest classifier is trained. With the same set of features we achieve 88.6% accuracy for user identification. Previous research [19] shows that gait information such as stride length and cadence are good features for person identification. Our result further demonstrates that even a small piece of pressure matrix, whose dimension is not enough to cover two footsteps, is already enough to identify people based on their weight, feet size and their way of interaction with furniture.

These results suggest that different postures and actions affect the weight balance on the floor. From this information the pressure matrix is able to tell which person is interacting with which furniture in the 3D space.

4.2.4. Smart-TableCloth for nutrition monitoring

Monitoring caloric intake and eating habits is a highly relevant problem for which there is yet no clear approach. Current solutions that provide accurate nutrition monitoring tend to be highly obtrusive (e.g. electrodes attached to neck [77]), while unobtrusive solutions remain inaccurate in terms of information they provide (e.g. wrist worn accelerometers [78], wearable cameras [79], and in-ear microphones [80]). As an additional sensing modality, we integrated a 30×42 textile pressure matrix with 1 cm^2 spatial resolution onto the top of a dining tablet and 4 Force Sensitive Resistors (FSR) at the corners under the tablet for diet monitoring (see Fig. 9) [81]. This application demonstrates the ability to detect very subtle pressure changes that propagate from the human body through numerous objects (cutlery, plate).

The system was evaluated with help of 10 healthy subjects, each having consumed a total of 8 meals chosen from 17 possible main dishes with 6 possible side dishes and a glass of water. We defined 8 classes that are common actions while eating with fork, knife and spoon: *Stirr* (Noodles), *Scoop solid* (Rice), *Cut* (Steak), *Poke/pierce* (Nuggets), *Scoop liquid* (Soup), *Poke/collect* (Salad), *Remove/Replace* (Water glass), and *No action*. The latter class indicates chewing or talking breaks when the user is not touching the plates.

To simulate a real dining session the participants were asked to eat as they normally would. Only western cutlery was used. The participants were not restricted by specific cutlery for the different types of meals, e.g. some used fork and knife to collect the salad while other used a spoon. They were also allowed to watch TV or talk during their meal. The dining sessions lasted between 15 and 40 min each, depending on the participants' eating habits. The experiments were video recorded and labelled manually.

Each pressure image is first up-sampled from 30×42 to 60×84. Atherton and Kerbysons's circle detection algorithm [69] is then applied to build bounding boxes around the plates and glasses, which leave circular footprints underneath. Based on these boxes the image is segmented into 3 regions, each containing one of the 3 food/water containers. For each region the average weight and the centre of weight are calculated.

In total 68 time and frequency domain features are calculated for each labelled action. We trained a confidence based AdaBoost algorithm (ConfAdaBoost.M1), which is a recently developed variant of the popular Adaboost.M1 classifier [82]. By performing a person dependent 10-fold cross validation with balanced classes we can classify 8 eating related actions with 90% accuracy. In the person independent case the average accuracy drops to 77%. This, however, is expected since there is a large variation in personal eating habits. When fusing information from the FSRs, the accuracy goes further up to 94% (person dependent). Spotting in the continuous data stream and estimation of food weight is also possible which we showed in previous work [81].

The dining tablet is able to unobtrusively spot and recognise basic actions that are related to food intake with fine granularity. The sensor can be used to estimate the eating speed and overall weight and if the user drinks enough water during the meal. This is valuable for evaluating long term eating habits that can be important in detecting changes in dietary patterns.

5. Discussion and conclusion

To explore surface based textile pressure sensing as a novel sensing modality for activity recognition, we developed general hardware architecture and data processing workflow. We also demonstrated their feasibility via 5 representative application scenarios. In these scenarios, the Smart-Surface is highly non-obtrusive and provides detailed pressure distribution, which is hard to detect with other sensing systems. The Smart-Surface is also multi-functional on two levels: the same hardware implementation can give multiple information (e.g. both upper body activity and the person's identity as a floor) and be used in multiple scenarios (e.g. the same piece of textile can be put on a table for nutrition monitoring, or on sofa as an input interface). These 5 applications are just the foundation of our exploration. For the future we plan to explore the following issues:

Study on textile properties: Existing studies have shown that textile sensors suffer from non-linearity, drifting and hysteresis [7,8]. We observed the same phenomenon in experiments with our design. In our current applications, we are looking at activities which generate short-time high pressure changes, so the changing pattern and the overall distribution play a more important role for activity recognition than the absolute pressure value at each single point. However, in some applications, direct measuring of weight might be favourable. For example, the user might benefit from a sport-mat which also measures the precise body-weight or a table-cloth which also measures the dish weight. We are planning to perform a detailed evaluation of textile (both physical model and electronic performance) regarding its non-linearity, drifting, hysteresis and their changes after multiple times of washing.

Real-time recognition and feedback: Data are now processed off-line on a computer which stores the data. In applications like gym-exercises, live feedback would be very helpful. Because image analysis is based on matrix calculations, it could be greatly accelerated using parallel data processing on an FPGA. After that, on-line data recognition and real-time wireless information exchange with other devices like mobile phones might become possible.

Wearable application exploration: All the 5 application scenarios are ambient. Pressure sensor matrices placed on-body could also reveal much details on pressure generated by muscle movement, body posture or direct user input. We have started exploration in this direction and a smart textile based platform combining resistive pressure sensing and other sensing modalities is already working [83].

Context-aware and self adaptation: In each scenario of the 5 scenarios, the Smart-Surface was used only for one major purpose. We assume the system knows the context, thus where it is and for what purpose it is used. To be genuine multi-functional, the system should be able to discover the context and select proper data processing algorithms by itself.

Fusion with other sensing modalities: We investigated fusion in the nutrition monitoring scenario with 2 formats of pressure sensing, namely the Smart-Surface and distinct FSR's. Fusing with other sensors (both wearable and ambient) could further improve the recognition.

Super large-scale matrix for group activity recognition: In all scenarios, there is only one subject at a time using the system. As humans are social beings, analysis of their relations and interactions is of great interest. Our architecture allows $\sim 10^6$ channels within one system. By expanding the current implementation from $\sim 10^4$ channels to $\sim 10^6$, exploration on group activity application becomes possible.

Based on the explored applications and with the potentially possible improvements, we believe that Smart-Surface can be a useful novel sensing modality, which opens new possibilities for future activity recognition applications.

Acknowledgement

References

[1] M. Sundholm, J. Cheng, B. Zhou, A. Sethi, P. Lukowicz, Smart-mat: Recognizing and counting gym exercises with low-cost resistive pressure sensing matrix, in: Proceedings of the 2014 ACM International Joint Conference on Pervasive and Ubiquitous Computing, ACM, 2014, pp. 373–382.

[2] J. Cheng, M. Sundholm, B. Zhou, M. Kreil, P. Lukowicz, Recognizing subtle user activities and person identity with cheap resistive pressure sensing carpet, in: 2014 International Conference on Intelligent Environments (IE), IEEE, 2014, pp. 148–153.

[3] B. Zhou, J. Cheng, M. Sundholm, A. Reiss, W. Huang, O. Amft, P. Lukowicz, Smart table surface: A novel approach to pervasive dining monitoring, in: 2015 IEEE International Conference on Pervasive Computing and Communications (PerCom), IEEE, 2015, pp. 155–162.

[4] J. Cheng, M. Sundholm, M. Hirsch, B. Zhou, S. Palacio, P. Lukowicz, Application exploring of ubiquitous pressure sensitive matrix as input resource for home-service robots, in: Robot Intelligence Technology and Applications 3, Springer, 2015, pp. 359–371.

[5] L. Shu, T. Hua, Y. Wang, Q. Li, D.D. Feng, X. Tao, In-shoe plantar pressure measurement and analysis system based on fabric pressure sensing array, IEEE Trans. Inf. Technol. Biomed. 14 (3) (2010) 767–775.

[6] W. Xu, M-C. Huang, N. Amini, J.J. Liu, L. He, M. Sarrafzadeh, Smart insole: a wearable system for gait analysis, in: Proceedings of the 5th International Conference on PErvasive Technologies Related to Assistive Environments, ACM, 2012, p. 18.

[7] J. Meyer, B. Arnrich, J. Schumm, G. Tröster, Design and modeling of a textile pressure sensor for sitting posture classification, IEEE Sens. J. 10 (8) (2010) 1391–1398.

[8] W. Xu, M-C. Huang, N. Amini, L. He, M. Sarrafzadeh, eCushion: A textile pressure sensor array design and calibration for sitting posture analysis, IEEE Sens. J. 13 (10) (2013) 3926–3934.

[9] H.Z. Tan, L. Slivovsky, A. Pentland, et al., A sensing chair using pressure distribution sensors, IEEE/ASME Trans. Mechatronics 6 (3) (2001) 261–268.

[10] X. Xie, B. Zheng, W. Xue, Object identification on car seat based on rough sets, in: 2011 IEEE 3rd International Conference on Communication Software and Networks, 2011, pp. 157–159.

[11] J.-H. Lim, H. Jang, J. Jang, S.-J. Park, Daily activity recognition system for the elderly using pressure sensors, in: Engineering in Medicine and Biology Society, 2008. EMBS 2008. 30th Annual International Conference of the IEEE, IEEE, 2008, pp. 5188–5191.

[12] M-C. Huang, J.J. Liu, W. Xu, N. Alshurafa, X. Zhang, M. Sarrafzadeh, Using pressure map sequences for recognition of on bed rehabilitation exercises, IEEE J. Biomed. Health Inform. 18 (2) (2014) 411–418.

[13] J.J. Liu, W. Xu, M-C. Huang, N. Alshurafa, M. Sarrafzadeh, N. Raut, B. Yadegar, Sleep posture analysis using a dense pressure sensitive bedsheet, Pervasive Mob. Comput. 10 (2014) 34–50.

[14] L. Samy, M-C. Huang, J.J. Liu, W. Xu, M. Sarrafzadeh, Unobtrusive sleep stage identification using a pressure-sensitive bed sheet, IEEE Sens. J. 14 (7) (2014) 2092–2101.

[15] D. Savio, T. Ludwig, Smart carpet: A footstep tracking interface, in: 21st International Conference on Advanced Information Networking and Applications Workshops, 2007, AINAW'07. Vol. 2, IEEE, 2007, pp. 754–760.

[16] Y. Kaddoura, J. King, A.S. Helal, Cost-precision tradeoffs in unencumbered floor-based indoor location tracking, in: 3rd International Conference on Smart Homes and Health Telematics, Sherbrooke, Québec, Canada, 2005, pp. 75–82.

[17] L. Middleton, A. Buss, A. Bazin, M.S. Nixon, et al., A floor sensor system for gait recognition, in: Fourth IEEE Workshop on Automatic Identification Advanced Technologies, 2005, IEEE, 2005, pp. 171–176.

[18] R.J. Orr, G.D. Abowd, The smart floor: a mechanism for natural user identification and tracking, in: CHI'00 Extended Abstracts on Human Factors in Computing Systems, ACM, 2000, pp. 275–276.

[19] G. Qian, J. Zhang, A. Kidané, People identification using gait via floor pressure sensing and analysis, in: Smart Sensing and Context, Springer, 2008, pp. 83–98.

[20] P. Srinivasan, D. Birchfield, G. Qian, A. Kidané, A pressure sensing floor for interactive media applications, in: Proceedings of the 2005 ACM SIGCHI International Conference on Advances in Computer Entertainment Technology, ACM, 2005, pp. 278–281.

[21] S. Rangarajan, A. Kidané, G. Qian, S. Rajko, Design Optimization of Pressure Sensing Floor for Multimodal Human–Computer Interaction, INTECH Open Access Publisher, 2008.

[22] B.-D.H. GesmbH. Boot-doc official website, http://www.boot-doc.com/analyse-systeme/einlagen-fraese (last access: August 2015).

[23] A. Bränzel, C. Holz, D. Hoffmann, D. Schmidt, M. Knaust, P. Lühne, R. Meusel, S. Richter, P. Baudisch, Gravityspace: tracking users and their poses in a smart room using a pressure-sensing floor, in: Proceedings of the SIGCHI Conference on Human Factors in Computing Systems, ACM, 2013, pp. 725–734.

[24] S.P. INC., Tactilus—real-time surface pressure mapping technology, 2015. URL: http://www.sensorprod.com/tactilus.php.

[25] S. De Rossi, T. Lenzi, N. Vitiello, M. Donati, A. Persichetti, F. Giovacchini, F. Vecchi, M. Carrozza, Development of an in-shoe pressure-sensitive device for gait analysis, in: Engineering in Medicine and Biology Society, EMBC, 2011 Annual International Conference of the IEEE, IEEE, 2011, pp. 5637–5640.

[26] E. Marenzi, R. Lombardi, G.M. Bertolotti, A. Cristiani, B. Cabras, Design and development of a novel capacitive sensor matrix for measuring pressure distribution, in: Sensors Applications Symposium (SAS), 2012 IEEE, IEEE, 2012, pp. 1–6.

[27] J.M. Kortelainen, M. van Gils, J. Parkka, Multichannel bed pressure sensor for sleep monitoring, in: Computing in Cardiology (CinC), 2012, IEEE, 2012, pp. 313–316.

[28] S. Lokavee, T. Puntheeranurak, T. Kerdcharoen, N. Watthanwisuth, A. Tuantranont, Sensor pillow and bed sheet system: Unconstrained monitoring of respiration rate and posture movements during sleep, in: 2012 IEEE International Conference on Systems, Man, and Cybernetics (SMC), IEEE, 2012, pp. 1564–1568.

[29] D.S. Tawil, D. Rye, M. Velonaki, Improved image reconstruction for an eit-based sensitive skin with multiple internal electrodes, IEEE Trans. Robot. 27 (3) (2011) 425–435.

[30] H.S. INC., Using an i/o port pin as an a/d converter input. URL: http://www.holtek.com/english/tech/appnote/uc/pdf/ha0128e.pdf.

[31] D.S. Holder, Electrical Impedance Tomography: Methods, History and Applications, CRC Press, 2004.

[32] E.M. Tapia, S.S. Intille, K. Larson, Activity Recognition in the Home Using Simple and Ubiquitous Sensors, Springer, 2004.

[33] J.R. Kwapisz, G.M. Weiss, S.A. Moore, Activity recognition using cell phone accelerometers, ACM SigKDD Explor. Newslett. 12 (2) (2011) 74–82.

[34] S.-W. Lee, K. Mase, Activity and location recognition using wearable sensors, IEEE Pervasive Comput. 1 (3) (2002) 24–32.

[35] C. Ramos, J.C. Augusto, D. Shapiro, Ambient intelligence—the next step for artificial intelligence, IEEE Intell. Syst. 23 (2) (2008) 15–18.

[36] N. Ravi, N. Dandekar, P. Mysore, M.L. Littman, Activity recognition from accelerometer data, in: AAAI, Vol. 5, 2005, pp. 1541–1546.

[37] H. Junker, O. Amft, P. Lukowicz, G. Tröster, Gesture spotting with body-worn inertial sensors to detect user activities, Pattern Recognit. 41 (6) (2008) 2010–2024.

[38] Fitbit: One & Zip Wireless Activity & Sleep Tracker, 2015. URL: http://www.fitbit.com.

[39] U. Maurer, A. Rowe, A. Smailagic, D. Siewiorek, Location and activity recognition using ewatch: A wearable sensor platform, in: Ambient Intelligence in Everyday Life, Springer, 2006, pp. 86–102.

[40] R. McNaney, J. Vines, D. Roggen, M. Balaam, P. Zhang, I. Poliakov, P. Olivier, Exploring the acceptability of google glass as an everyday assistive device for people with Parkinson's, in: Proceedings of the 32nd Annual ACM Conference on Human Factors in Computing Systems, ACM, 2014, pp. 2551–2554.

[41] S. Rhee, B.-H. Yang, K. Chang, H.H. Asada, The ring sensor: a new ambulatory wearable sensor for twenty-four hour patient monitoring, in: Engineering in Medicine and Biology Society, 1998. Proceedings of the 20th Annual International Conference of the IEEE, Vol. 4, IEEE, 1998, pp. 1906–1909.

[42] J.A. Ward, P. Lukowicz, G. Troster, T.E. Starner, Activity recognition of assembly tasks using body-worn microphones and accelerometers, IEEE Trans. Pattern Anal. Mach. Intell. 28 (10) (2006) 1553–1567.

[43] P. Lukowicz, F. Hanser, C. Szubski, W. Schobersberger, Detecting and interpreting muscle activity with wearable force sensors, Lecture Notes in Comput. Sci. 3968 (2006) 101–116.

[44] R. Wimmer, M. Kranz, S. Boring, A. Schmidt, A capacitive sensing toolkit for pervasive activity detection and recognition, in: Fifth Annual IEEE International Conference on Pervasive Computing and Communications, 2007. PerCom'07, IEEE, 2007, pp. 171–180.

[45] M. Stäger, P. Lukowicz, G. Tröster, Power and accuracy trade-offs in sound-based context recognition systems, Pervasive Mob. Comput. 3 (3) (2007) 300–327.

[46] G. Pirkl, K. Stockinger, K. Kunze, P. Lukowicz, Adapting magnetic resonant coupling based relative positioning technology for wearable activitiy recogniton, in: 12th IEEE International Symposium on Wearable Computers, 2008. ISWC 2008, IEEE, 2008, pp. 47–54.

[47] X. Jiang, C.-J.M. Liang, K. Chen, B. Zhang, J. Hsu, J. Liu, B. Cao, F. Zhao, Design and evaluation of a wireless magnetic-based proximity detection platform for indoor applications, in: Proceedings of the 11th International Conference on Information Processing in Sensor Networks, ACM, 2012, pp. 221–232.

[48] C. Occhiuzzi, S. Cippitelli, G. Marrocco, Modeling, design and experimentation of wearable RFID sensor tag, IEEE Trans. Antennas and Propagation 58 (8) (2010) 2490–2498.

[49] P. Bonato, et al., Wearable sensors/systems and their impact on biomedical engineering, IEEE Eng. Med. Biol. Mag. 22 (3) (2003) 18–20.

[50] R. Bodor, R. Morlok, N. Papanikolopoulos, Dual-camera system for multi-level activity recognition, in: IROS, Citeseer, 2004, pp. 643–648.

[51] P. Hevesi, S. Wille, G. Pirkl, N. Wehn, P. Lukowicz, Monitoring household activities and user location with a cheap, unobtrusive thermal sensor array, in: Proceedings of the 2014 ACM International Joint Conference on Pervasive and Ubiquitous Computing, ACM, 2014, pp. 141–145.

[52] J. Han, B. Bhanu, Human activity recognition in thermal infrared imagery, in: IEEE Computer Society Conference on Computer Vision and Pattern Recognition-Workshops, 2005. CVPR Workshops, IEEE, 2005, 17–17.

[53] L. Xia, C.-C. Chen, J.K. Aggarwal, Human detection using depth information by kinect, in: 2011 IEEE Computer Society Conference on Computer Vision and Pattern Recognition Workshops (CVPRW), IEEE, 2011, pp. 15–22.

[54] T. Hori, K. Aizawa, Context-based video retrieval system for the life-log applications, in: Proceedings of the 5th ACM SIGMM International Workshop on Multimedia Information Retrieval, ACM, 2003, pp. 31–38.

[55] G. Bauer, K. Stockinger, P. Lukowicz, Recognizing the use-mode of kitchen appliances from their current consumption, in: EuroSSC, Springer, 2009, pp. 163–176.

[56] J. Chen, A.H. Kam, J. Zhang, N. Liu, L. Shue, Bathroom activity monitoring based on sound, in: Pervasive Computing, Springer, 2005, pp. 47–61.

[57] F. Naya, H. Noma, R. Ohmura, K. Kogure, Bluetooth-based indoor proximity sensing for nursing context awareness, in: Ninth IEEE International Symposium on Wearable Computers, 2005. Proceedings, IEEE, 2005, pp. 212–213.

[58] A. Steinhage, C. Lauterbach, Sensfloor and navifloor: Large area sensor systems beneath your feet, in: Handbook of Research on Ambient Intelligence and Smart Environments: Trends and Perspectives 2, 2011, pp. 41–55.

[59] G.D. Abowd, E.D. Mynatt, Designing for the human experience in smart environments, in: Smart Environments: Technologies, Protocols, and Applications, 2005, pp. 151–174.

[60] J. Pansiot, D. Stoyanov, D. McIlwraith, B.P. Lo, G.-Z. Yang, Ambient and wearable sensor fusion for activity recognition in healthcare monitoring systems, in: 4th International Workshop on Wearable and Implantable Body Sensor Networks (BSN 2007), Springer, 2007, pp. 208–212.

[61] B. Zhou, J. Cheng, M. Sundholm, P. Lukowicz, From smart clothing to smart table cloth: Design and implementation of a large scale, textile pressure matrix sensor, in: Architecture of Computing Systems–ARCS 2014, Springer, 2014, pp. 159–170.

[62] SEFAR, Sefar official website, http://www.sefar.com (last access: August 2015).

[63] SEFAR, Sefar carbontex, http://techlist.sefar.com/cms/newtechlistpdf.nsf/vwWebPDFs/carbotex_EN.pdf (last access: August 2015).

[64] S. Balakrishnama, A. Ganapathiraju, Linear discriminant analysis-a brief tutorial, Institute for Signal and information Processing.

[65] R.G. Keys, Cubic convolution interpolation for digital image processing, IEEE Trans. Acoust. Speech Signal Process. 29 (6) (1981) 1153–1160.

[66] M.-K. Hu, Visual pattern recognition by moment invariants, IRE Trans. Inform. Theory 8 (2) (1962) 179–187.

[67] M.R. Teague, Image analysis via the general theory of moments*, J. Opt. Soc. Amer. 70 (8) (1980) 920–930.

[68] A. Khotanzad, Y.H. Hong, Invariant image recognition by zernike moments, IEEE Trans. Pattern Anal. Mach. Intell. 12 (5) (1990) 489–497.

[69] T.J. Atherton, D.J. Kerbyson, Size invariant circle detection, Image Vis. Comput. 17 (11) (1999) 795–803.

[70] H. Ng, S. Ong, K. Foong, P. Goh, W. Nowinski, Medical image segmentation using k-means clustering and improved watershed algorithm, in: 2006 IEEE Southwest Symposium on Image Analysis and Interpretation, IEEE, 2006, pp. 61–65.

[71] J. Goldberger, H. Greenspan, S. Gordon, Unsupervised image clustering using the information bottleneck method, in: Pattern Recognition, Springer, 2002, pp. 158–165.

[72] H. Sakoe, S. Chiba, Dynamic programming algorithm optimization for spoken word recognition, IEEE Trans. Acoust. Speech Signal Process. 26 (1) (1978) 43–49.

[73] W. El Falou, J. Duchêne, M. Grabisch, D. Hewson, Y. Langeron, F. Lino, Evaluation of driver discomfort during long-duration car driving, Appl. Ergon. 34 (3) (2003) 249–255.

[74] Y. Choi, J. Park, B. Lee, K. Jung, S. Sah, H. You, A classification of sitting strategies based on seating pressure distribution, J. Korean Inst. Indust. Eng. 39 (2) (2013) 105–108.

[75] Mayo clinic fitness multimedia, 2014. URL: http://www.mayoclinic.org/healthy-living/fitness/multimedia/HLV-20049447?s=9.

[76] C. Goutte, E. Gaussier, A probabilistic interpretation of precision, recall and f-score, with implication for evaluation, in: Advances in Information Retrieval, Springer, 2005, pp. 345–359.

[77] M. Farooq, J.M. Fontana, E. Sazonov, A novel approach for food intake detection using electroglottography, Physiol. Meas. 35 (5) (2014) 739.

[78] O. Amft, D. Bannach, G. Pirkl, M. Kreil, P. Lukowicz, Towards wearable sensing-based assessment of fluid intake, in: 2010 8th IEEE International Conference on Pervasive Computing and Communications Workshops (PERCOM Workshops), IEEE, 2010, pp. 298–303.

[79] M. Puri, Z. Zhu, Q. Yu, A. Divakaran, H. Sawhney, Recognition and volume estimation of food intake using a mobile device, in: 2009 Workshop on Applications of Computer Vision (WACV), IEEE, 2009, pp. 1–8.

[80] J. Nishimura, T. Kuroda, Eating habits monitoring using wireless wearable in-ear microphone, in: 3rd International Symposium on Wireless Pervasive Computing, 2008. ISWPC 2008, IEEE, 2008, pp. 130–132.

[81] B. Zhou, J. Cheng, P. Lukowicz, A. Reiss, O. Amft, Monitoring dietary behavior with a smart dining tray, IEEE Pervasive Comput. 14 (4) (2015) 46–56.

[82] A. Reiss, G. Hendeby, D. Stricker, Confidence-based multiclass adaboost for physical activity monitoring, in: Proceedings of the 2013 International Symposium on Wearable Computers, ACM, 2013, pp. 13–20.

[83] S. Schneegass, M. Hassib, B. Zhou, J. Cheng, F. Seoane, O. Amft, P. Lukowicz, A. Schmidt, Simpleskin: towards multipurpose smart garments, in: Proceedings of the 2015 ACM International Joint Conference on Pervasive and Ubiquitous Computing and Proceedings of the 2015 ACM International Symposium on Wearable Computers, ACM, 2015, pp. 241–244.